Journal of Trace Elements in Medicine and Biology 62 (2020) 126555

Contents lists available at ScienceDirect

Journal of Trace Elements in Medicine and Biology

journal homepage: www.elsevier.com/locate/jtemb

# Analysis of neuronal iron deposits in Parkinson's disease brain tissue by synchrotron x-ray spectromicroscopy

Jake Brooks[a,*,1], James Everett[a,b,1], Frederik Lermyte[a,c], Vindy Tjendana Tjhin[a], Peter J. Sadler[c], Neil Telling[b], Joanna F. Collingwood[a]

[a] School of Engineering, University of Warwick, Coventry CV4 7AL, UK
[b] School of Pharmacy and Bioengineering, Keele University, Stoke-on-Trent ST4 7QB, UK
[c] Department of Chemistry, University of Warwick, Coventry CV4 7EQ, UK

ARTICLE INFO

*Keywords:*
Parkinson's disease
Iron
Oxidation state
Soft x-ray
Spectromicroscopy
Synchrotron

ABSTRACT

*Background:* Neuromelanin-pigmented neurons, which are highly susceptible to neurodegeneration in the Parkinson's disease substantia nigra, harbour elevated iron levels in the diseased state. Whilst it is widely believed that neuronal iron is stored in an inert, ferric form, perturbations to normal metal homeostasis could potentially generate more reactive forms of iron capable of stimulating toxicity and cell death. However, non-disruptive analysis of brain metals is inherently challenging, since use of stains or chemical fixatives, for example, can significantly influence metal ion distributions and/or concentrations in tissues.

*Aims:* The aim of this study was to apply synchrotron soft x-ray spectromicroscopy to the characterisation of iron deposits and their local environment within neuromelanin-containing neurons of Parkinson's disease substantia nigra.

*Methods:* Soft x-ray spectromicroscopy was applied in the form of Scanning Transmission X-ray Microscopy (STXM) to analyse resin-embedded tissue, without requirement for chemically disruptive processing or staining. Measurements were performed at the oxygen and iron *K*-edges in order to characterise both organic and inorganic components of anatomical tissue using a single label-free method.

*Results:* STXM revealed evidence for mixed oxidation states of neuronal iron deposits associated with neuromelanin clusters in Parkinson's disease substantia nigra. The excellent sensitivity, specificity and spatial resolution of these STXM measurements showed that the iron oxidation state varies across sub-micron length scales.

*Conclusions:* The label-free STXM approach is highly suited to characterising the distributions of both inorganic and organic components of anatomical tissue, and provides a proof-of-concept for investigating trace metal speciation within Parkinson's disease neuromelanin-containing neurons.

## 1. Introduction

Many neurodegenerative disorders are associated with altered metal ion metabolism in the brain [1]. In Parkinson's disease (PD), iron levels are significantly elevated in the type of nerve cell most severely compromised by disease progression – the dopaminergic neurons within the substantia nigra pars compacta (SNc) region [2]. Death of these vulnerable dopamine-producing neurons ultimately leads to a severe depletion of striatal dopamine, inducing the characteristic symptoms of PD such as tremor, rigidity and bradykinesia. Although trace metals are essential for normal physiological brain function, localised perturbations to metal homeostasis could potentially be responsible for initiating toxicity and region-specific cell death [3–5]. Thus, it is critical to develop methods capable of characterising changes in metal chemistry at a subcellular level.

The high rate of oxidative metabolism and augmented iron concentrations leave the brain particularly susceptible to oxidative stress [6]. Whilst redox switching between ferric ($Fe^{3+}$) and ferrous ($Fe^{2+}$) forms is key to iron's functional role in neurotransmitter synthesis, myelin synthesis and cellular metabolism [3], these reactions can also generate reactive oxygen species which are highly toxic to cells *via* Fenton and related redox chemistry [3,7]. Strict regulatory systems

* Corresponding author.
*E-mail address:* J.Brooks.1@warwick.ac.uk (J. Brooks).
[1] These authors contributed equally.

https://doi.org/10.1016/j.jtemb.2020.126555
Received 24 January 2020; Received in revised form 9 May 2020; Accepted 15 May 2020

must be appropriately maintained to ensure a sufficient supply of iron for essential processes whilst protecting vulnerable neurons from iron-mediated toxicity.

Whilst the iron storage protein, ferritin, is the dominant iron sink in glial cells of the SNc, iron in nigral neurons is primarily bound by the biological polymer, neuromelanin (NM) [8,9]. NM pigments dopaminergic neurons of the SNc and noradrenergic neurons in the locus coeruleus, the two brain regions most susceptible to neuron loss during the progression of PD [10]. Similar to ferritin, NM also sequesters ferrous iron and binds it in a redox-stabilised ferric form, forming iron oxide clusters which comprise around 10%–20% of total iron in the substantia nigra [11]. It has been proposed that the antioxidant defences offered by iron-binding molecules such as ferritin and NM may be impaired by the ageing process, thereby increasing vulnerability towards age-related neurodegeneration. [3,12]. Moreover, it is possible that the storage capacity of these iron reservoirs may be particularly compromised in PD, leading to hazardous levels of redox-active iron contained within, or in the immediate vicinity of vulnerable neurons [13–15].

Despite the potential implications for disease-specific iron dysregulation in PD, there has only been limited exploration of interactions between iron and NM in PD substantia nigra using high-resolution spectromicroscopy [16]. This is chiefly because non-disruptive, label-free analysis of brain metals poses significant inherent analytical challenges, whereas use of stains or chemical fixatives can significantly influence metal ion distributions and/or concentrations in tissues [17–19]. Synchrotron-based techniques to study subcellular structure and chemistry in disease pathology are consequently of current interest [20], since these methods can be applied without sample ablation or requirement for additional staining (*i.e.* they are label-free) [21]. Recent developments in soft x-ray synchrotron techniques represent a pivotal advancement in this field, allowing inorganic metal distributions to be visualised with respect to organic, anatomical tissue structure.

Scanning Transmission X-ray Microscopy (STXM) is one such synchrotron-based, soft x-ray approach, particularly suited to providing combined imaging and spectral data on biological tissue samples. In STXM, the energy of the incident beam can be precisely tuned and stepped over a desired range to generate x-ray absorption spectra over a targeted absorption edge (*e.g.* carbon or iron *K*-edges). The high energy resolution attainable with STXM (*ca.* 0.1 eV) promotes sensitivity towards chemical variations in the sample, allowing speciation of endogenous metal ions. Image contrast can also be generated by exploiting distinct spectral features to create speciation maps, illustrating not only the distribution of individual elements, but the distribution of specific molecules and ions (*e.g.* proteins, $Fe^{2+}/Fe^{3+}$). This powerful analytical tool has previously been applied to perform specific mapping of organic tissue components [21] and to advance understanding of Alzheimer's disease aetiology, characterising interactions between metal ions and the amyloid-beta peptide in both *in vitro* [22–24] and *ex vivo* [25] studies.

The aim of this study was to apply STXM to the characterisation of iron deposits and their local environment within neuromelanin-containing neurons of Parkinson's disease SNc. Combined imaging and spectral data were used to demonstrate the heterogeneous structure and composition of post-mortem brain tissue samples, whilst also detecting variations in the oxidation state of neuronal iron.

## 2. Materials and methods

### 2.1. Tissue preparation

Frozen unfixed substantia nigra tissue from a confirmed PD case was obtained from the Canadian Brain Tissue Bank and prepared and analysed under current ethical approvals 07/MRE08/12 and REGO-2018-2223.

Substantia nigra tissue was cut into cubes approximately 8 $mm^3$ in volume using a non-metallic knife to prevent metal contamination, and dehydrated using an ethanol series (40%–100% dry). Following dehydration, tissue cubes were embedded in an aliphatic epoxy resin composed of an equimolar mixture of trimethylolpropane triglycidyl ether and 4,4′-methylenebis-(2-methylcyclohexylamine), purchased from Sigma Aldrich (Dorset, UK), and cured at 60 °C overnight.

Prior work demonstrated that ferric iron standards prepared using the same embedding series as for the substantia nigra tissue show no evidence of iron reduction when examined using STXM [26]. Thus, whilst the absolute concentrations of loosely-bound metal ions may be altered by the resin-embedding process, it is likely that iron oxidation state is preserved.

For soft x-ray spectromicroscopy (STXM) experiments, semi-thin, 500 nm thick sections of resin embedded substantia nigra tissue were cut using a Reichert-Jung ultra-cut microtome, operating with a diamond blade (DiATOME Ultra 45°). Sections were mounted on copper TEM grids for STXM examination. No dyes or contrast agents were applied.

### 2.2. Scanning transmission X-ray microscopy

STXM experiments were performed on Diamond Light Source beamline I08 (Oxfordshire, UK), and the Advanced Light Source beamline 11.0.2 (Berkeley, CA, USA). Microscopy images were obtained by tuning the incident x-ray beam to a specific energy, raster scanning the sample across a focussed beam of $<$ 50 nm spot size, and recording the transmitted X-ray intensity. Exposure times were kept to a minimum ($\leq$ 10 ms per point) to prevent radiation damage.

Speciation maps showing the nanoscale distribution of particular elements or chemical states were generated by collecting paired images: a "peak" image at the energy corresponding to a feature of interest (*e.g.* the principal $Fe^{3+}$ $L_3$-edge peak at 709.5 eV), and an "off-peak" image a few eV below this feature. The off-peak image was then subtracted from the peak image providing a speciation map devoid of artefacts (from for example, the embedding resin). Speciation maps were created for features at the oxygen *K*-edge ($520-545$ eV) and the iron $L_3$-edge ($700-716$ eV).

Iron $L_3$-edge x-ray absorption spectra, providing detailed information regarding the oxidation state of the measured iron deposits, were obtained by collecting images of a region of interest at multiple x-ray energies across the absorption edge. Normalisation of the x-ray absorption spectra was achieved by converting the raw x-ray absorption intensity to optical density using background regions that did not contain any iron material (*e.g.* areas of the resin that are devoid of tissue). The "dark count", *i.e.* the background noise attributable to the beamline, was determined by acquiring a single image with no incident x-ray beam and subtracted from the stack before conversion to optical density. By performing this form of spectromicroscopy, x-ray absorption spectra can be generated from each pixel of an image, allowing the iron oxidation state from highly localised ($<$ 50 nm) regions of interest to be determined. A three-point average smoothing was applied to all iron $L_3$-edge x-ray absorption spectra collected.

STXM data processing was performed using the aXis 2000 software package (http://unicorn.mcmaster.ca/aXis2000.html). Pseudo-coloured composite images were created by converting greyscale images to false colour, before recombining the images as an overlay using ImageJ.

The data that support the findings in this study will be available in the Warwick Research Archive Portal (WRAP) repository, https://wrap.warwick.ac.uk/137342.

## 3. Results

STXM images, speciation maps and an iron $L_3$-edge x-ray absorption spectrum from a neuromelanin-containing neuron within an embedded

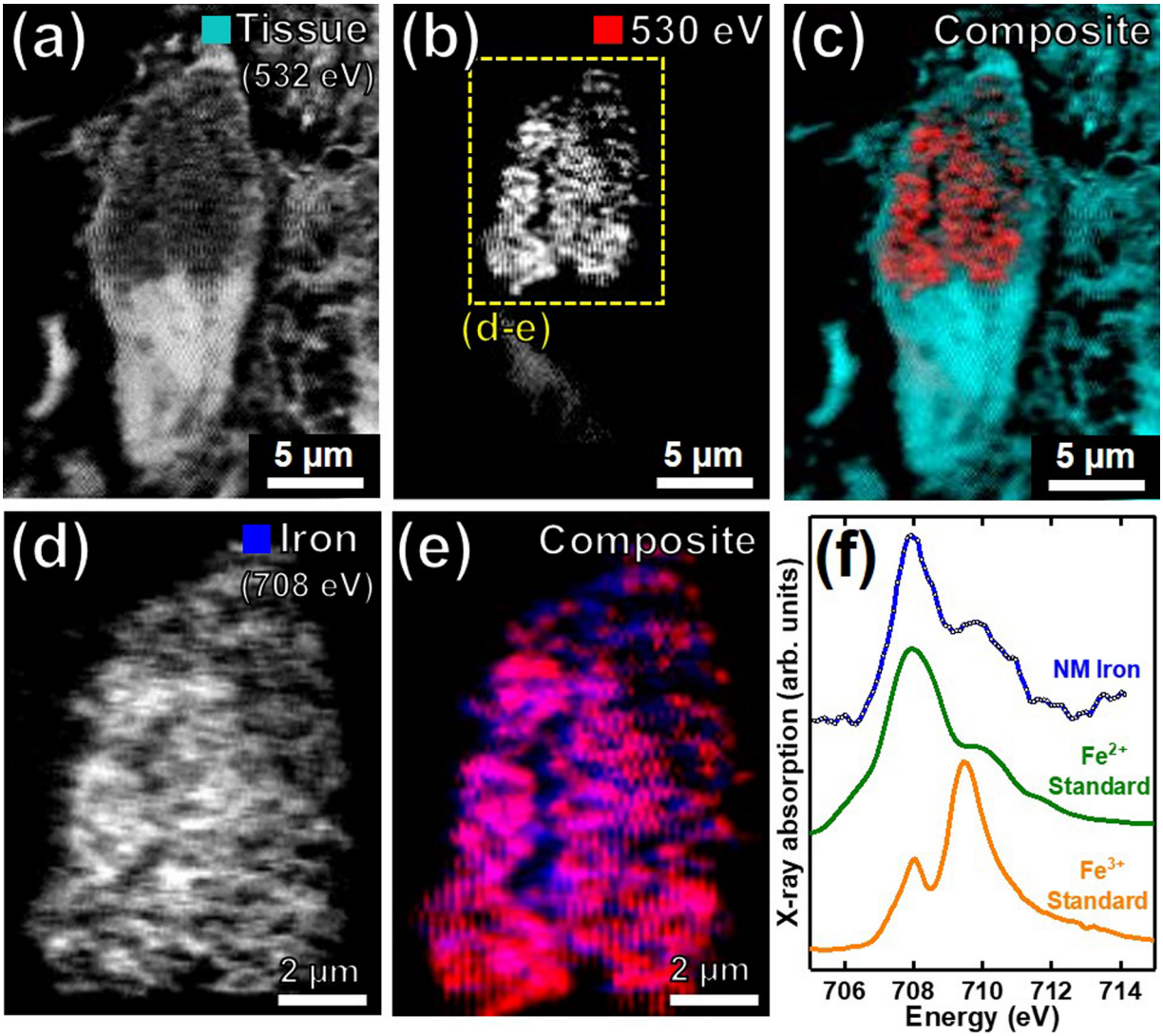


**Fig. 1.** X-ray speciation maps, images, and an iron $L_3$-edge x-ray absorption spectrum from a neuromelanin-containing neuron within a PD substantia nigra tissue section. (a) Oxygen *K*-edge tissue map. (b) Off-peak 530 eV image, showing NM granules as areas of strong contrast. (c) Composite image displaying tissue (cyan) and NM (red) content. (d) Iron $L_3$-edge speciation map and (e) composite image displaying iron (blue) and NM (red), from the area highlighted in (b). (f) Iron $L_3$-edge spectrum (blue) from the NM area shown in (d). Ferric ($Fe^{3+}$; orange) and ferrous ($Fe^{2+}$; green) standard spectra are also provided for reference. (For interpretation of the references to colour in this figure legend, the reader is referred to the web version of this article).

section of PD substantia nigra are shown in Fig. 1. An oxygen *K*-edge speciation map taken at 532 eV, displaying tissue ultrastructure, is shown in Fig. 1a. From this map a clear cell border and intracellular structure can be seen. An off-resonance 530 eV image is shown in Fig. 1b, in which an intracellular cluster of NM is visible as a region of high contrast, owing to NM's higher optical density compared to the surrounding neuropil at this energy. Iron $L_3$-edge mapping of the neuron at 709.5 eV (Fig. 1d), showed a cellular iron distribution which closely matches that of NM (Fig. 1b and e), suggesting that NM is loaded with iron.

To establish the oxidation state of the NM-associated iron, x-ray spectromicroscopy was performed over the iron $L_3$-edge. At the $L_3$-edge, ferric ($Fe^{3+}$) materials display a principal absorption peak at 709.5 eV and a further low intensity peak at 708 eV (for reference spectrum see Fig. 1f; orange spectrum). In contrast, pure ferrous ($Fe^{2+}$) materials display a single peak at 708 eV (see Fig. 1f; green spectrum). Therefore, increases in the $Fe^{2+}$ content of an originally ferric material result in an increased peak intensity at 708 eV with respect to the feature at 709.5 eV. The iron $L_3$-edge x-ray absorption spectrum from the NM-associated iron (Fig. 1f; blue spectrum) strongly resembled the ferrous standard, demonstrating this iron to be predominantly $Fe^{2+}$.

A STXM image and iron $L_3$-edge x-ray absorption spectra from a further NM cluster located within the same tissue section are shown in Fig. 2. In the 709.5 eV image (Fig. 2a), a large $>$ 15 µm diameter cluster of NM is evident, within which individual NM granules ($<$ 600 nm diameter) can be resolved.

Iron $L_3$-edge x-ray absorption spectra from five individual NM granules are shown in Fig. 2b. Even within nanoscale regions, a clear variation in iron oxidation state can be seen in the different NM granules. The spectra from the areas labelled B1–B2 are characteristic of an $Fe^{3+}$ phase. In contrast, spectra B3→B5 displayed increased $Fe^{2+}$ features, as evidenced by the enhancement of the feature at 708 eV in relation to the principal $Fe^{3+}$ peak at 709.5 eV, and are plotted in ascending order with regards to their $Fe^{2+}$ content. These results again show the presence of chemically reduced iron associated with NM in PD substantia nigra, and suggest that the degree of reduction can vary between adjacent NM granules.

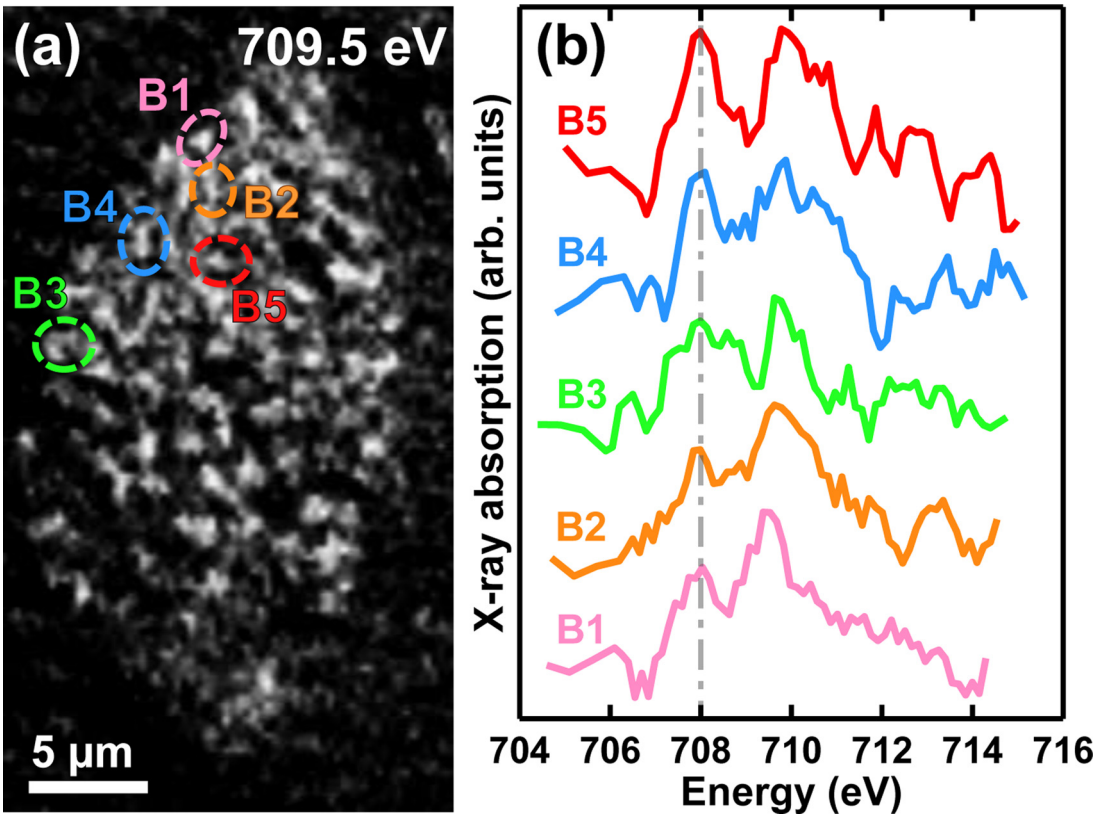


**Fig. 2.** (a) An iron $L_3$-edge x-ray image and (b) x-ray absorption spectra from NM granules in a PD substantia nigra tissue section, demonstrating nanoscale variation in iron oxidation state. X-ray spectra in (b) correspond to the areas highlighted in (a). The dotted-dashed line at 708 eV in (b) indicates the peak absorption energy for $Fe^{2+}$.

## 4. Discussion

Despite the association between elevated iron levels and PD having been recognised for nearly a century, the mechanisms linking iron dysregulation and neurotoxicity are not yet fully understood, and it remains unclear as to why dopaminergic neurons in the SNc are so heavily affected by neurodegeneration, whilst other iron-rich nuclei are spared [13].

This work demonstrates that STXM is a powerful tool for analysing NM clusters and associated iron distributions within neuromelanin-containing neurons, without requirement for chemically disruptive staining. The ability to characterise metal ion distributions in context with the surrounding anatomical tissue structure without labelling offers unique potential to investigate the native chemistry of tissue samples *in situ*. This is particularly pertinent to analysis of vulnerable neuromelanin-containing neurons in the PD substantia nigra, where elevated iron levels have consistently been reported [2,27,28].

The positive identification of NM was informed by related recently-published work confirming the utility of STXM for label-free imaging of NM [21]. Spectral features shared by NM clusters and synthetic NM were used to create speciation maps demonstrating equivalent distributional information to that obtained from silver nitrate staining in consecutive tissue sections [21]. Because STXM signal relies on energy-dependent x-ray transmission through the resin-embedded tissue sections, and on analyte concentration at a specific absorption edge, the prior NM labelling work was optimised at the lower-energy carbon *K*-edge in thinner (200 nm) sections. In the present study, thicker 500 nm sections were used to maximise iron signal for the chemical speciation of NM-associated iron. In these 500 nm sections we confirmed that the off-resonance signal near the oxygen edge (530 eV, Fig. 1) evidences sufficient contrast from the NM clusters that the NM distribution and chemical speciation of NM-associated iron could be studied in a single section, as illustrated here. NM granules were distinguished by their characteristic granular morphology and increased optical density relative to surrounding cellular ultrastructure at the oxygen *K*-edge. We note that both the morphology and surrounding cellular context of large intracellular neuromelanin clusters were entirely consistent with large intracellular neuromelanin clusters observed previously using silver nitrate labelling, or optimised carbon *K*-edge STXM mapping [21].

We show that x-ray spectromicroscopy using STXM provides sufficiently high spatial resolution and chemical sensitivity to allow acquisition of x-ray absorption spectra from individual NM granules. Dense clusters of NM approximately 300 − 500 nm in diameter are shown to be loaded with iron, consistent with the well-documented high affinity of NM for metal ions [29–31]. Nanoscale variations in iron oxidation state were observed amongst NM granules, highlighting the need for nanoscale spatial resolution when examining the biochemistry of tissue samples, whilst also drawing attention to the remarkable specificity of STXM for speciation analysis.

Destructive microprobe techniques such as laser ablation inductively coupled plasma mass spectrometry (LA-ICP-MS) have been utilised effectively for the purpose of quantifying metal concentrations in targeted regions of tissue [32,33]. Whilst such techniques are ideally suited to quantification and can certainly achieve exceptional chemical sensitivity, the capacity to distinguish different metal oxidation states or to measure regions on the nanoscale is lacking [34]. STXM can elucidate metal speciation on the nanoscale, whilst also preserving the sample for complementary analysis. The ability to acquire large volumes of data from small volumes of sample is particularly important to post-mortem tissue studies, where sample supply is necessarily constrained [35].

With iron typically stored in a ferric ($Fe^{3+}$) state within NM granules, the presence of chemically reduced iron is certainly intriguing with regards to the hypothesis that the antioxidant metal-binding

function of NM may be compromised by ageing, or even specifically in Parkinson's disease [13–15]. NM-bound iron clusters measured with identical x-ray doses showed both ferric and ferrous-rich forms of iron. We have previously shown that such effects are not caused by artefacts such as x-ray beam reduction [25]; therefore, the localised variation in iron oxidation state supports the possibility of redox cycling between ferric ($Fe^{3+}$) and ferrous ($Fe^{2+}$) ions, potentially accompanied by generation of toxic species such as free radicals.

Redox cycling of metal ions (including iron, manganese and copper) may be instrumental in exacerbating oxidative stress in the brain, a mechanism which is receiving growing attention concerning its association with neurodegeneration and ageing in general [4,36–38]. The results shown here provide proof-of-concept using tissue from a single PD case. The highly localised variations in iron oxidation state within neuromelanin-containing neurons clearly warrants further investigation, to incorporate additional PD casesand neurologically healthy controls.

In summary, we demonstrate that soft x-ray spectromicroscopy using STXM offers a level of information which would normally demand extensive application of multiple complementary techniques, each requiring independent sample preparation. The detection of signals for both organic and inorganic components, combined with the high spatial resolution, specificity, and sensitivity for trace metal detection, makes STXM a powerful method for in-depth studies of disrupted biochemistry in the PD brain.

## CRediT authorship contribution statement

**Jake Brooks:** Conceptualization, Methodology, Validation, Formal analysis, Investigation, Writing - original draft. **James Everett:** Conceptualization, Methodology, Validation, Formal analysis, Investigation, Writing - original draft. **Frederik Lermyte:** Conceptualization, Investigation, Methodology, Writing - review & editing. **Vindy Tjendana Tjhin:** Investigation, Methodology. **Peter J. Sadler:** Writing - review & editing, Project administration, Funding acquisition. **Neil Telling:** Conceptualization, Methodology, Software, Investigation, Writing - review & editing, Supervision, Project administration, Funding acquisition. **Joanna F. Collingwood:** Conceptualization, Investigation, Resources, Writing - review & editing, Supervision, Project administration, Funding acquisition.

## Declaration of Competing Interest

The authors declare that they have no known competing financial interests or personal relationships that could have appeared to influence the work reported in this paper.

## Acknowledgments

This work was supported by EPSRC grants EP/N033191/1, EP/N033140/1, EP/K035193/1, and an EPSRC Doctoral Training Award to J.B (EP/N509796/1). Human brain tissue used in this study was analysed in accordance with the Declaration of Helsinki under the remit of ethical approvals REGO-2018-2223 from the BSREC at University of Warwick, and approval 07/MRE08/12 from the North West Haydock Ethics Committee. Human tissue was obtained with informed consent from the Canadian Brain Tissue Bank, with thanks to Dr L.N. Hazrati for assisting with tissue provision. We thank Diamond Light Source for access to beamline I08 (proposal SP15230) and Dr T. Araki, Dr M. Kazemian Abyaneh and Dr B. Kaulich for technical assistance at the beamline. We also thank the Advanced Light Source for access to beamline 11.0.2 to collect synchrotron data presented in this study. The Advanced Light Source is a DOE Office of Science User Facility under contract no. DE-AC02-05CH11231.

## References

[1] H. Kozlowski, A. Janicka-Klos, J. Brasun, E. Gaggelli, D. Valensin, G. Valensin, Copper, iron, and zinc ions homeostasis and their role in neurodegenerative disorders (metal uptake, transport, distribution and regulation), Coord. Chem. Rev. 253 (21-22) (2009) 2665–2685.
[2] A.E. Oakley, et al., Individual dopaminergic neurons show raised iron levels in Parkinson disease, Neurology 68 (21) (2007) 1820–1825.
[3] A.A. Belaidi, A.I. Bush, Iron neurochemistry in Alzheimer's disease and Parkinson's disease: targets for therapeutics, J. Neurochem. 139 (2016) 179–197.
[4] P. Dusek, P.M. Roos, T. Litwin, S.A. Schneider, T.P. Flaten, J. Aaseth, The neurotoxicity of iron, copper and manganese in Parkinson's and Wilson's diseases, J. Trace Elem. Med. Biol. 31 (2015) 193–203.
[5] D. Berg, et al., Brain iron pathways and their relevance to Parkinson's disease, J. Neurochem. 79 (2) (2001) 225–236.
[6] J. Connor, K. Boeshore, S. Benkovic, S. Menzies, Isoforms of ferritin have a specific cellular distribution in the brain, J. Neurosci. Res. 37 (4) (1994) 461–465.
[7] J.K. Andersen, Oxidative stress in neurodegeneration: cause or consequence? Nat. Med. 10 (7s) (2004) S18.
[8] L. Zecca, et al., Iron, neuromelanin and ferritin content in the substantia nigra of normal subjects at different ages: consequences for iron storage and neurodegenerative processes, J. Neurochem. 76 (6) (2001) 1766–1773.
[9] J. Connor, S. Menzies, S.S. Martin, E. Mufson, Cellular distribution of transferrin, ferritin, and iron in normal and aged human brains, J. Neurosci. Res. 27 (4) (1990) 595–611.
[10] L. Zecca, D. Tampellini, M. Gerlach, P. Riederer, R.G. Fariello, D. Sulzer, Substantia nigra neuromelanin: structure, synthesis, and molecular behaviour, Mol. Pathol. Rev. 54 (6) (2001) 414–418.
[11] J.F. Collingwood, N.D. Telling, Iron oxides in the human brain, in: D. Faivre (Ed.), Iron Oxides: From Nature to Materials and from Formation to Applications, first ed., John Wiley & Sons, Weinheim, Germany, 2016ch. 7..
[12] G.A. Salvador, Iron in neuronal function and dysfunction, Biofactors 36 (March-April 2) (2010) 103–110, https://doi.org/10.1002/biof.80.
[13] D.J. Hare, K.L. Double, Iron and dopamine: a toxic couple, Brain 139 (4) (2016) 1026–1035.
[14] M.E. Götz, K. Double, M. Gerlach, M.B. Youdim, P. Riederere, The relevance of iron in the pathogenesis of Parkinson's disease, Ann. N. Y. Acad. Sci. 1012 (1) (2004) 193–208.
[15] L. Lopiano, et al., Q-band EPR investigations of neuromelanin in control and Parkinson's disease patients, Biochim. Biophys. Acta Mol. Basis Dis. 1500 (3) (2000) 306–312.
[16] A. Biesemeier, et al., Elemental mapping of neuromelanin organelles of human substantia nigra: correlative ultrastructural and chemical analysis by analytical transmission electron microscopy and nano-secondary ion mass spectrometry, J. Neurochem. 138 (2) (2016) 339–353.
[17] G. Robison, et al., X-ray fluorescence imaging: a new tool for studying manganese neurotoxicity, PLoS One 7 (11) (2012) e48899.
[18] D.J. Hare, et al., The effect of paraformaldehyde fixation and sucrose cryoprotection on metal concentration in murine neurological tissue, J. Anal. At. Spectrom. 29 (3) (2014) 565–570.
[19] G. Robison, B. Sullivan, J.R. Cannon, Y. Pushkar, Identification of dopaminergic neurons of the substantia nigra pars compacta as a target of manganese accumulation, Metallomics 7 (5) (2015) 748–755.
[20] A. Sakdinawat, D. Attwood, Nanoscale X-ray imaging, Nat. Photonics 4 (12) (2010) 840.
[21] J. Brooks, et al., Label-free nanoimaging of Neuromelanin in the brain by Soft x-ray spectromicroscopy, Angew. Chem. Int. Ed. (2020), https://doi.org/10.1002/anie.202000239.
[22] F. Lermyte, et al., Emerging approaches to investigate the influence of transition metals in the proteinopathies, Cells 8 (10) (2019) 1231.
[23] J. Everett, et al., Evidence of redox-active Iron formation following aggregation of ferrihydrite and the alzheimer's disease peptide beta-amyloid, (in english), Inorg. Chem. 53 (March 6) (2014) 2803–2809, https://doi.org/10.1021/ic402406g.
[24] J. Everett, et al., Ferrous iron formation following the co-aggregation of ferric iron and the Alzheimer's disease peptide β-amyloid (1–42), J. R. Soc. Interface 11 (95) (2014) 20140165.
[25] J. Everett, et al., Nanoscale synchrotron X-ray speciation of iron and calcium compounds in amyloid plaque cores from Alzheimer's disease subjects, Nanoscale 10 (2018) 11782–11796.
[26] N.D. Telling, et al., Iron biochemistry is correlated with amyloid plaque morphology in an established mouse model of alzheimer's disease, Cell Chem. Biol. 24 (October 10) (2017) 1205–1215, https://doi.org/10.1016/j.chembiol.2017.07.014.
[27] E. Sofic, et al., Increased iron (III) and total iron content in post mortem substantia nigra of parkinsonian brain, J. Neural Transm. 74 (3) (1988) 199–205.
[28] M. Gerlach, K. Double, M. Youdim, P. Riederer, Potential sources of increased iron in the substantia nigra of parkinsonian patients, J. Neural Transm. Suppl. (2006) 133–142.
[29] L. Zecca, et al., The neuromelanin of human substantia nigra and its interaction with metals, J. Neural Transm. 109 (5-6) (2002) 663–672.
[30] F.A. Zucca, et al., Interactions of iron, dopamine and neuromelanin pathways in brain aging and Parkinson's disease, Prog. Neurobiol. 155 (2017) 96–119, https://doi.org/10.1016/j.pneurobio.2015.09.012.
[31] W.S. Enochs, T. Sarna, L. Zecca, P.A. Riley, H.M. Swartz, The roles of neuromelanin, binding of metal ions, and oxidative cytotoxicity in the pathogenesis of Parkinson's disease: a hypothesis, J. Neural Transm. 7 (2) (1994) 83–100.

[32] J. Sabine Becker, Imaging of metals in biological tissue by laser ablation inductively coupled plasma mass spectrometry (LA-ICP-MS): state of the art and future developments, J. Mass Spectrom. 48 (February 2) (2013) 255–268, https://doi.org/10.1002/jms.3168.

[33] J.S. Becker, A. Matusch, C. Palm, D. Salber, K.A. Morton, J.S. Becker, Bioimaging of metals in brain tissue by laser ablation inductively coupled plasma mass spectrometry (LA-ICP-MS) and metallomics, Metallomics 2 (2) (2010) 104–111.

[34] J.F. Collingwood, F. Adams, Chemical imaging analysis of the brain with X-ray methods, Spectrochim. Acta Part B At. Spectrosc. 130 (2017) 101–118.

[35] J.F. Collingwood, M.R. Davidson, The role of iron in neurodegenerative disorders: insights and opportunities with synchrotron light, Front. Pharmacol. 5 (2014) 191, https://doi.org/10.3389/fphar.2014.00191.

[36] E. Monzani, et al., Dopamine, oxidative stress and protein–Quinone modifications in parkinson's and other neurodegenerative diseases, Angew. Chem. 58 (20) (2019) 6512–6527.

[37] R.J. Ward, D.T. Dexter, R.R. Crichton, Neurodegenerative diseases and therapeutic strategies using iron chelators, J. Trace Elem. Med. Biol. 31 (2015) 267–273, https://doi.org/10.1016/j.jtemb.2014.12.012.

[38] Z. Yarjanli, K. Ghaedi, A. Esmaeili, S. Rahgozar, A. Zarrabi, Iron oxide nanoparticles may damage to the neural tissue through iron accumulation, oxidative stress, and protein aggregation, BMC Neurosci. 18 (1) (2017) 51.